

Seeking better times: atomic clocks in the generalized Tonks-Girardeau regime

S. V. Mousavi,^{1,*} A. del Campo,^{2,†} I. Lizuain,^{2,‡} M. Pons,^{3,§} and J. G. Muga^{2,¶}

¹Department of Physics, Sharif University of Technology, P. O. Box 11365-9161, Tehran, Iran

²Departamento de Química-Física, UPV-EHU, Apartado. 644, Bilbao, Spain

³Departamento de Física Aplicada I, E.U.I.T. de Minas y Obras Públicas, UPV-EHU, 48901 Barakaldo, Spain

This article is based on the talk with the same title at the Blaubeuren meeting. First we discuss briefly the importance of time and time keeping, explaining the basic functioning of clocks in general and atomic clocks in particular, which rely on Ramsey interferometry. The usefulness of cold atoms is discussed as well as their limits in Bose-Einstein condensates. An alternative that we study is a different cold-atom regime: the Tonks-Girardeau (TG) gas of tightly confined and strongly interacting bosons. The TG gas is reviewed and then generalized for two-level atoms. Finally, we explore the combination of Ramsey interferometry and TG gases.

PACS numbers:

I. INTRODUCTION

It is hardly necessary to insist on the practical importance of time since we all live attached to a time machine, the wrist watch, which organizes of our daily routine. For running a Conference as in Blaubeuren, a precision of one minute is enough, but for plenty of activities fundamental to modern society a much more precise time keeping is necessary: banks, electric power companies, telecommunications, or GPS use atomic clocks.

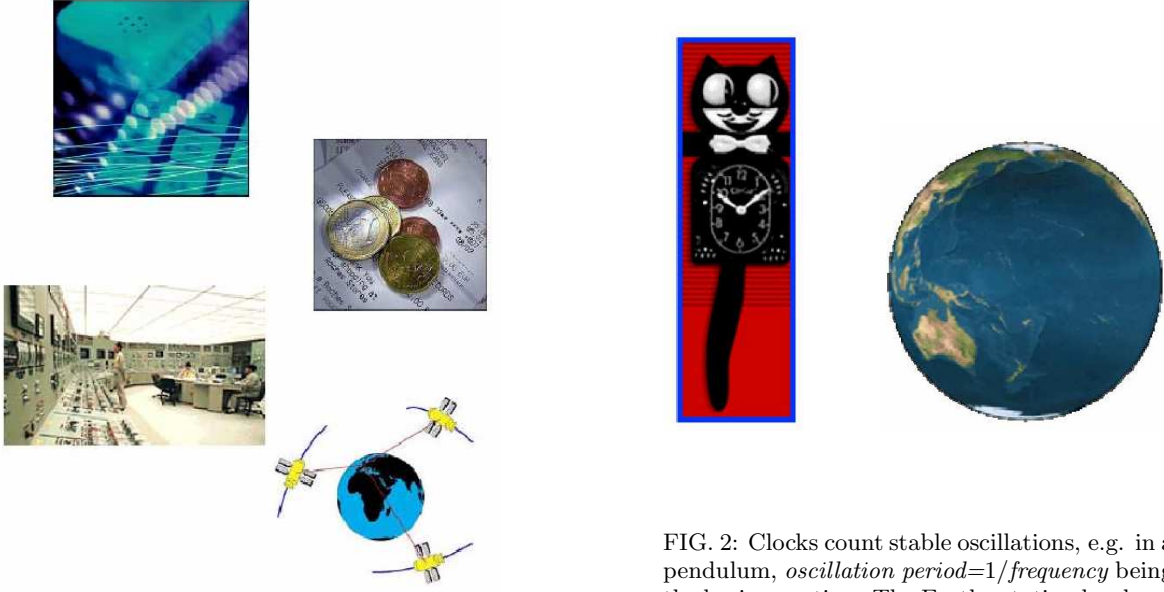


FIG. 1: Banking transactions, electric power companies, telecommunications and GPS need atomic clocks.

FIG. 2: Clocks count stable oscillations, e.g. in a pendulum, $oscillation\ period = 1/frequency$ being the basic equation. The Earth rotation has been the master clock for centuries but its speed is not constant!

A clock is a device that, in a sense, “produces” time, by counting stable oscillations (as in a pendulum, see the

*Electronic address: s.v.moosavi@mehr.sharif.edu

†Electronic address: adolfo.delcampo@ehu.es

‡Electronic address: ion.lizuain@ehu.es

§Electronic address: marisa.pons@ehu.es

¶Electronic address: jg.muga@ehu.es

quantum-cat clock of Fig. 2). Clocks of many different types have been used along history by different civilizations but the Earth rotation has been for centuries the master clock. Nevertheless, we know nowadays that the rotation speed may be affected by a series of physical phenomena, such as tidal friction, which slows down the earth at a non-negligible pace in the geological scale (a poor dinosaur had to rush for a sandwich in stressful days of 23 hours); even the accumulation of snow on top of the mountains in the winters of the Northern hemisphere may affect the rotation speed -by conservation of angular momentum- making winter days indeed longer than summer days. If we kept the definition of the second attached to the actual Earth's rotation, we should also change the laws of physics from summer to winter, and add proper correction terms to account for tidal friction. This sounds very unreasonable. Instead, we could also try to correct for these perturbing effects “by hand”, but unfortunately not all the perturbations are easy to predict or understand (e.g., those due to magma motion), so corrections using other astronomical periods were tried, but they were very cumbersome to handle, and not stable enough anyway. Fortunately nature has a lot of stability to offer in the opposite direction, in the world of the small.

Atomic clocks, in particular, count the oscillations of the field resonant with an atomic transition, most frequently a hyperfine transition of caesium-133 (which defines officially the second as the time required for 9192631770 periods of the resonant microwave field). An external quartz oscillator is locked by a servo loop to a resonance excitation curve between two hyperfine states $|g\rangle$ and $|e\rangle$ so that its frequency is always adjusted to the maximum of the curve, and thus to the natural frequency of the selected transition.

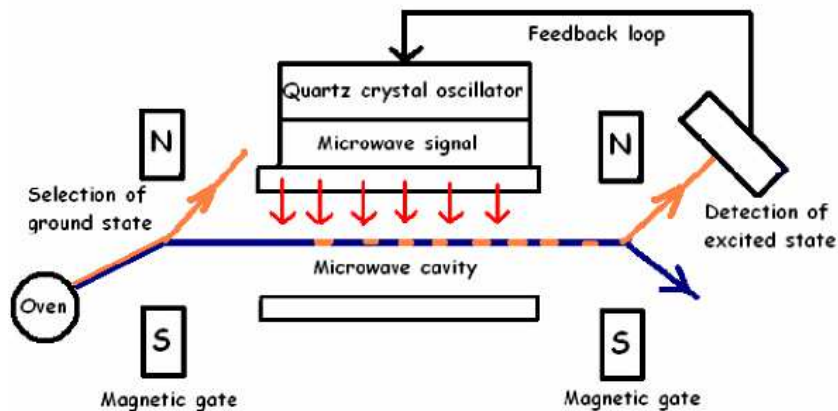


FIG. 3: Principle of an atomic clock based on a “Rabi”, or one-cavity scheme. Deflection angles are greatly exaggerated. Actual clocks operate usually with two separated cavities (“Ramsey scheme”).

In more detail, see Fig. 3, caesium atoms are heated in an oven to produce a beam. A first magnet filters out the excited atoms so that only ground state atoms enter into the microwave cavity in which the field wavevector is perpendicular to the atomic motion, and the frequency, locked to an external quartz oscillator, is very close to the transition frequency. This excites some atoms which are selected with a second magnet and later detected. The excitation probability compared with previous runs at slightly different frequencies tells us how far or close is the field frequency to the transition frequency, and this information is used to modify the excitation frequency so that it stays as closely as possible to the maximum of the excitation curve, see Fig. 4. The clock includes the appropriate counting electronics which we shall not discuss here. A very sharp peak is clearly desirable to minimize the fluctuation of the external oscillation frequency around the natural one. This contributes to the stability of the clock and explains why a beam configuration is chosen: a perpendicular excitation with respect to the atomic motion avoids the Doppler effect and its associated line broadening.

In actual clocks things are slightly more complicated because instead of a single cavity (Rabi scheme) there are actually two (Ramsey scheme). The reason for the two cavities is that they produce a quantum interference between two possible paths corresponding to excitation in the first cavity or excitation in the second, and this interference may be used to sharpen the resonance and to make it less dependent of or inhomogeneities of the fields. The Hamiltonian describing the process, assuming classical motion for the center of mass, is

$$H = \frac{\hat{p}^2}{2m} - \hbar\delta|e\rangle\langle e| + \frac{\hbar}{2}\Omega(\hat{x})(|g\rangle\langle e| + |e\rangle\langle g|), \quad (1)$$

where Ω is the Rabi frequency and δ the detuning (laser frequency minus transition frequency), see Fig. 5. Note that the first path does not pick up any extra phase during free flight between the fields but the second one does ($e^{i\delta T}$).

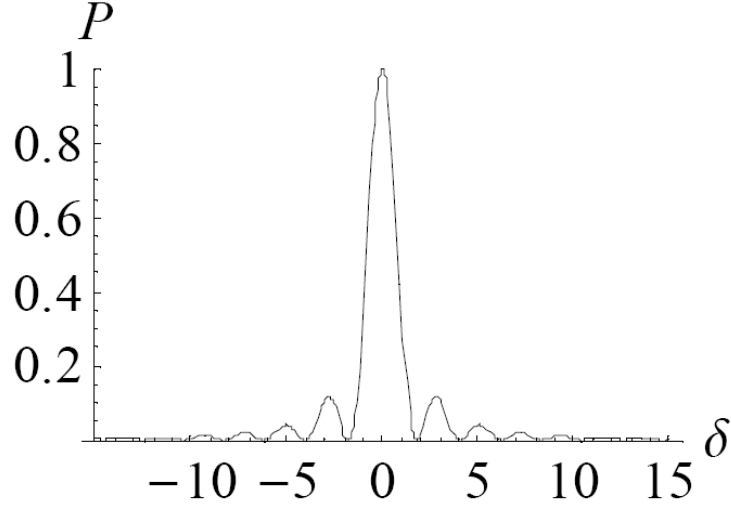


FIG. 4: An excitation probability curve versus detuning (arbitrary units).

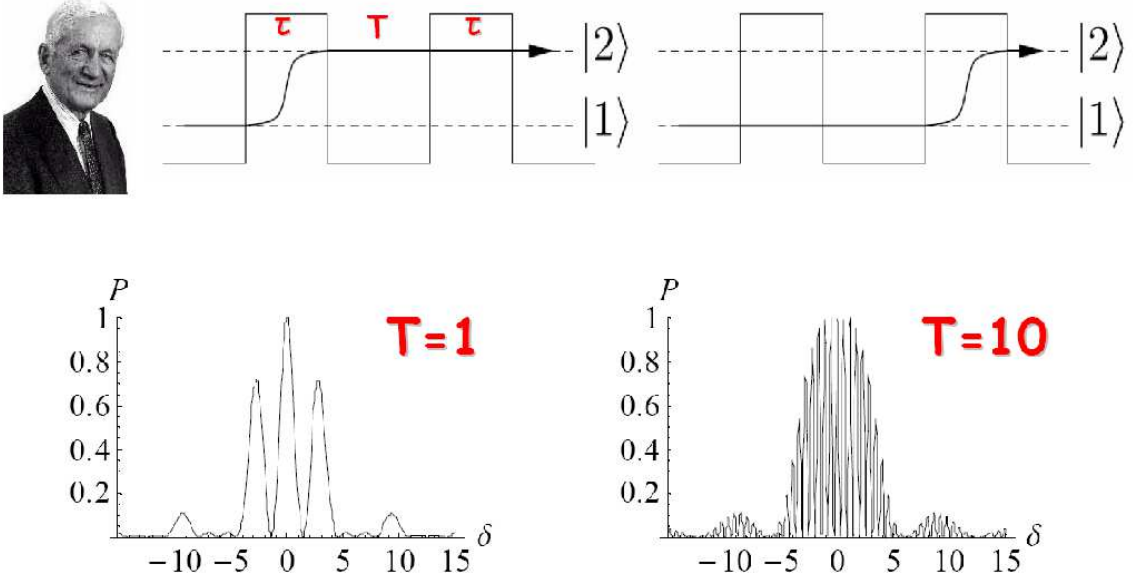


FIG. 5: Ramsey's method. The upper figures represent the two interfering paths. The lower figures illustrate the narrowing of the fringes when the free-flight time T between the two fields is increased.

The consequence is a final excitation probability proportional to $\cos^2(\delta T/2)$, which makes clear that longer free-flight times are desirable in order to achieve a narrower central fringe.

This motivates the use of cold atoms in time-frequency metrology. They are slow and big T 's may be produced, but other advantages exist: first they may reduce dramatically velocity broadening (the averaging of the fringes due to different velocities and times), and also they may lead to fundamentally new effects with coherent N-body states (e.g. entanglement has been proposed to beat quantum projection noise limit).

The use of a Bose-Einstein condensate for an atomic clock immediately comes to mind, but the improvements associated with low velocities and narrow velocity distribution may be compensated by negative effects, such as collisional shifts and instabilities leading to the separation of the gas cloud [12, 13].

A natural candidate for further exploration is the Tonks-Girardeau (TG) regime of impenetrable, tightly confined Bosons subjected to "contact" interactions [14, 15], since some of its properties are complementary to those of the condensates. In particular, the TG requirement of strong contact interactions, implies similarities between the

Bosonic system and a “dual” system of freely moving Fermions, with all local correlation functions and the elementary excitations of the TG Bosons and the dual system of Fermions being actually equal. Other important feature of the TG gas is its one dimensional (1D) character. Olshanii showed [16, 17, 18] that when a Bosonic vapor is confined in a wave guide with transverse trapping so tight and temperature so low that the transverse vibrational excitation quantum $\hbar\omega_\perp$ is larger than available longitudinal zero point and thermal energies, the effective dynamics becomes one dimensional, and accurately described by a 1D Hamiltonian with delta-function interactions $g_{1D}\delta(x_j - x_\ell)$, where x_j and x_ℓ are 1D longitudinal position variables. This is the Lieb-Liniger (LL) model, exactly solved in 1963 by a Bethe ansatz method [19]. The coupling constant g_{1D} can be tuned along a broad range of values by varying the magnetic field (and thus the three dimensional s-wave scattering length) or the confinement (confinement induced resonances) [16, 17]) near a Feshbach resonance; this allows in particular to reach the Tonks-Girardeau regime of impenetrable Bosons, which corresponds to the $g_{1D} \rightarrow \infty$ limit of the LL model. The limiting regime has been realized experimentally [20, 21], and was solved exactly in 1960 [14, 15] by the so called Fermi-Bose mapping to the ideal Fermi gas.

In metrology and atomic interferometry, the tight 1D confinement along a waveguide is a simplifying feature since no transversal motional branches have to be considered with the possible bonus of an increased signal. Nevertheless, the confinement is by itself problematic for frequency standard applications, since it is carried out by means of magnetic or optical interactions which will in principle perturb the internal state levels of the atom. Several schemes have been proposed to mitigate this problem and compensate or avoid the shifts due to magnetic [12] or optical interactions [22, 23], and we shall assume hereafter that such a compensation is implemented.

The possible applications in interferometry are a strong motivation for current research in TG gases. Interference effects have been examined so far in a few publications in which internal states have not played any role [24, 25]. Indeed, a TG model including internal states and an external interaction coupling them has not been discussed, although optically guided systems with free spin subjected to potentials for singlet and triplet interactions have been studied by means of effective LL models [26, 27]. Note also that a model applicable to a two-level LL gas coupled by an on-resonance laser has been solved by nested Bethe ansatz [28].

In this work, we investigate the implications in Ramsey interferometry of a model in the spirit of the original (structureless) TG gas but with internal structure. The idealized, strong contact interactions of the model allow to achieve essential solvability of the dynamical problem in the Ramsey two-field excitation setup by simple quadrature: the collisions are characterized by internal state and momentum exchange, which reduce to the usual impenetrable constraint for collisions in the same internal channel. The difficulties and somewhat extreme requirements to implement the generalized TG gas may have negative implications in metrology applications which will also be discussed.

We shall study different configurations for the two fields, both in space and time domains. They are conceptually different and the mathematical treatment is different too. For reasonable parameters, however, the results turn out to be very similar.

II. TWO-LEVEL TONKS-GIRARDEAU GAS WITH EXCHANGE, CONTACT INTERACTIONS

A. Notation and contact interactions

We shall propose here a generalization of the Tonks-Girardeau gas for two-level impenetrable atoms. First we shall need to review or introduce some notation and basic concepts. In one dimension the state of a single two-level atom may be written as a two-component “spinor”

$$\Phi_n(x_1) = \sum_{b=g,e} \phi_n^{(b)}(x_1)|b\rangle, \quad (2)$$

where $n = 1, 2, 3, \dots$ is a label to distinguish different spinors and b is a generic index for the internal bound state, which may be g (ground), or e (excited). (Remark 1: Note that in general g and e do not necessarily correspond to states with definite values of the component of the electronic spin in one direction, i.e., the word “spinor” is here synonym of “two-component wave vector”; Remark 2: the subindex n will later on correspond to states prepared as harmonic oscillator eigenstates of a longitudinal trap.) One-particle states may be combined to form two-particle ones with the form

$$\Phi_{nn'}(x_1, x_2) = \sum_{b,b'} \phi_n^{(b)}(x_1)\phi_{n'}^{(b')}(x_2)|bb'\rangle, \quad (3)$$

and similarly for more particles. The convention in $|bb'\rangle$ is that b is for particle 1 and b' for particle 2. This will in some equations be indicated even more explicitly adding a particle subscript to the internal state label, b_1, b_2 , etc.

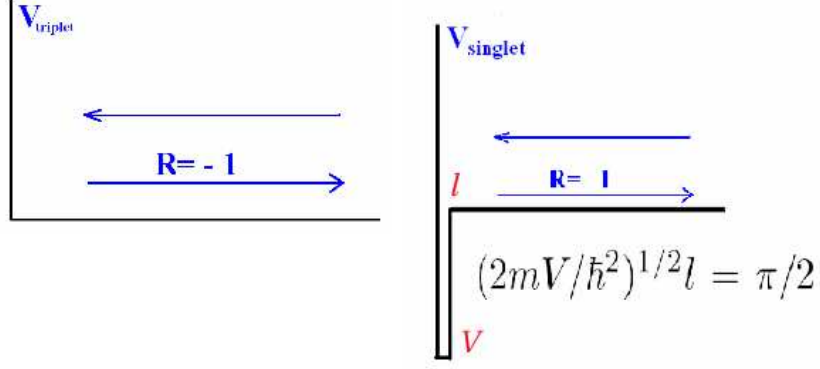


FIG. 6: Collisions for triplet and singlet potentials.

To discuss the contact interactions of the model consider now the usual Pauli operators acting on one-particle internal state vectors,

$$\begin{aligned}\sigma_X &= |g\rangle\langle e| + |e\rangle\langle g|, \\ \sigma_Y &= i(|g\rangle\langle e| - |e\rangle\langle g|), \\ \sigma_Z &= |e\rangle\langle e| - |g\rangle\langle g|,\end{aligned}\tag{4}$$

and the corresponding 3-component operator $\hat{\mathbf{S}}_j = \sigma_j/2$ for particle j analogous to the spin-1/2 angular momentum operator. If $\hat{\mathbf{S}} = \hat{\mathbf{S}}_1 + \hat{\mathbf{S}}_2$, $\hat{\mathbf{S}}^2$ has eigenvalues $S(S+1)$ with $S = 0$ and $S = 1$ corresponding to singlet and triplet subspaces spanned by $|-\rangle \equiv (|eg\rangle - |ge\rangle)/\sqrt{2}$ and $\{|gg\rangle, |ee\rangle, |+\rangle \equiv (|eg\rangle + |ge\rangle)/\sqrt{2}\}$ respectively.

Assume now the following Hamiltonian

$$\hat{H}_{\text{coll}} = -\frac{\hbar^2}{2m} \sum_{j=1}^2 \partial_{x_j}^2 + v_s(x_{12})\hat{P}_{12}^s + v_t(x_{12})\hat{P}_{12}^t.\tag{5}$$

Here $x_{12} = x_1 - x_2$, $\hat{P}_{12}^s = |-\rangle\langle -| = \frac{1}{4} - \hat{\mathbf{S}}_1 \cdot \hat{\mathbf{S}}_2$ is the projector onto the subspaces of singlet functions, and $\hat{P}_{12}^t = |gg\rangle\langle gg| + |ee\rangle\langle ee| + |+\rangle\langle +|$ is a projector onto the triplet subspace.

The internal Hilbert space can be written as the sum of singlet and triplet subspaces as $\mathcal{H}_s \oplus \mathcal{H}_t$. Suppose that the reflection amplitude for relative motion in such representation takes the values $+1, -1$ in singlet and triplet subspaces respectively. The particles are impenetrable and these values correspond to a hard wall potential v_t at $x_{12} = 0$ for all collisions in triplet channels $|gg\rangle \rightarrow |gg\rangle$, $|ee\rangle \rightarrow |ee\rangle$ or $|+\rangle \rightarrow |+\rangle$, whereas v_s has, in addition to the hard wall at $x_{12} = 0$, a well of width l and depth V , so that the reflection amplitude becomes $R = +1$ in the limit in which the well is made infinitely narrow and the well infinitely deep, keeping $(2mV/\hbar^2)^{1/2}l = \pi/2$ [26, 29, 30, 31]. (Notice that in these references the well applies to the triplet subspace and not to the singlet subspace as here. This -triplet-infinite well potential appears in the so called Fermionic Tonks-Girardeau gas [26, 29, 30].)

Translated into the g, e -basis and for the sector $x_1 < x_2$ this implies that in all collisions between atoms in g or e and well defined momenta, they interchange their momenta (the relative momentum changes sign), as well as their internal state, with the outgoing wave function picking up a minus sign because of the hard-core reflection, as shown in Fig. 7. For $x_1 < x_2$ and equal internal states such collision is represented by

$$e^{ikx_1}e^{ik'x_2}|bb\rangle - [e^{ik'x_1}e^{ikx_2}][bb],\tag{6}$$

whereas for $b \neq b'$,

$$e^{ikx_1}e^{ik'x_2}|bb'\rangle - [e^{ik'x_1}e^{ikx_2}][b'b].\tag{7}$$

In the diagonal case of equal internal states the spatial part vanishes at contact, $x_1 = x_2$, whereas in the non-diagonal case it does not, but note that in Eq. (7) only the “external region” is considered, disregarding the infinitely narrow well region.

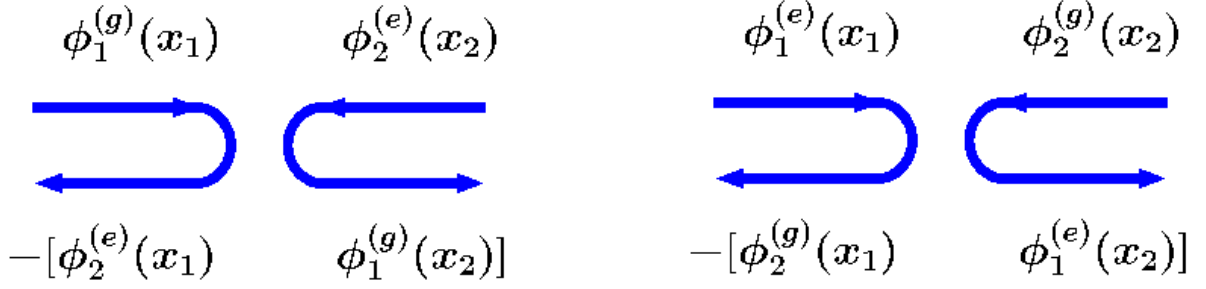


FIG. 7: Diagrammatic representation of the collisions for particles with different internal states in the sector $x_1 < x_2$: the particles interchange their momentum and internal state picking up an additional phase (minus sign).

We shall proceed now to discuss a possible implementation of these contact interactions. First of all, undesired inelastic collisions are expected to be substantially reduced by confinement at low collision energies, so as to limit the internal space to the two internal levels of the model and to the simple processes considered [32]. The internal levels of ^{133}Cs clocks, $|F=3, m_F=0\rangle$ and $|F=4, m_F=0\rangle$, combine spin-down and up components, and the different triplet elastic channels may have different scattering amplitudes. We may again rely on strong confinement and low energies to expect that the inner electronic cores will produce effective reflection coefficients close to -1 , independently of the internal state.

A second and important condition is the need to achieve strongly attractive singlet collisions. For two Bosons in the singlet subspace, the space wavefunction is antisymmetric, so that s-wave scattering is forbidden; therefore the interactions are governed to leading order by a 3D p-wave scattering amplitude and can be enhanced by a 1D odd-wave confinement-induced Feshbach resonance (CIR), which allows in principle to engineer v_s and achieve a strong attraction as required above. For two spin-polarized interacting Fermions [26, 29, 30, 33], the spatial symmetry of the subspaces is interchanged with respect to the Bosonic case, and one requires a p-wave scattering in the triplet subspace. However, in the rest of the paper we shall focus on the former, Bosonic case, whose dual, auxiliary system of free Fermions we introduce next.

B. Two noninteracting Fermions

Let us consider now a Fermionic state made of two noninteracting one-particle states with the form

$$\begin{aligned}\Psi_F(x_1, x_2) &= \frac{1}{\sqrt{2}} \begin{vmatrix} \Phi_1(x_1) & \Phi_1(x_2) \\ \Phi_2(x_1) & \Phi_2(x_2) \end{vmatrix} \\ &= \frac{1}{\sqrt{2}} \det_{n,j=1}^2 \Phi_n(x_j) \\ &= \frac{1}{\sqrt{2}} \sum_{b_1, b_2=g,e} \begin{vmatrix} \phi_1^{(b_1)}(x_1) & \phi_1^{(b_2)}(x_2) \\ \phi_2^{(b_1)}(x_1) & \phi_2^{(b_2)}(x_2) \end{vmatrix} |b_1 b_2\rangle,\end{aligned}$$

with the state sign changing by switching particles 1 and 2 *and* the internal states. We insist that these Fermions do not interact among themselves, but they could interact with an external potential as we shall see later. To construct the state we are simply combining two Hartree products of one-particle two-component wave-vectors Φ_n , each vector corresponding to the solution of the Schrödinger equation for a single Fermion with internal structure. Ψ_F is thus a solution of the Schrödinger equation for two Fermions without mutual interaction.

More explicitly,

$$\begin{aligned}2^{1/2}\Psi_F(x_1, x_2) &= \\ &+ [\phi_1^{(g)}(x_1)\phi_2^{(g)}(x_2) - \phi_2^{(g)}(x_1)\phi_1^{(g)}(x_2)]|gg\rangle \\ &+ [\phi_1^{(e)}(x_1)\phi_2^{(e)}(x_2) - \phi_2^{(e)}(x_1)\phi_1^{(e)}(x_2)]|ee\rangle \\ &+ [\phi_1^{(g)}(x_1)\phi_2^{(e)}(x_2) - \phi_2^{(g)}(x_1)\phi_1^{(e)}(x_2)]|ge\rangle \\ &+ [\phi_1^{(e)}(x_1)\phi_2^{(g)}(x_2) - \phi_2^{(e)}(x_1)\phi_1^{(g)}(x_2)]|eg\rangle\end{aligned}\tag{8}$$

It might at first be surprising that the spatial part for the non-diagonal components $|ge\rangle$ or $|eg\rangle$ does not vanish at $x_1 = x_2$, but one can check that the state is indeed Fermionic noticing that, with our notation, the interchange of particle label and internal state leaves in each term the internal state vectors $|bb'\rangle$ unchanged. Thus the interchange symmetry operation simply changes the sign of the total state.

C. Mapping to a Bosonic wave function

An associated Bosonic system of interacting atoms, totally symmetric under $(x_i, b_i) \leftrightarrow (x_j, b_j)$ permutations may be now obtained by means of the Bose-Fermi mapping, $\Psi_B(x_1, x_2) = \mathcal{A}\Psi_F(x_1, x_2)$, where the antisymmetric unit function is $\mathcal{A} = \text{sgn}(x_2 - x_1)$.

For the sector $x_1 < x_2$ we could use Eq. (8) directly, or rearrange it slightly to construct the Bosonic wave function as

$$\begin{aligned} 2^{1/2}\Psi_B(x_1, x_2) = & \\ & + [\phi_1^{(g)}(x_1)\phi_2^{(g)}(x_2) - \phi_2^{(g)}(x_1)\phi_1^{(g)}(x_2)]|gg\rangle \\ & + [\phi_1^{(e)}(x_1)\phi_2^{(e)}(x_2) - \phi_2^{(e)}(x_1)\phi_1^{(e)}(x_2)]|ee\rangle \\ & + [\phi_1^{(g)}(x_1)\phi_2^{(e)}(x_2)]|ge\rangle - [\phi_2^{(e)}(x_1)\phi_1^{(g)}(x_2)]|eg\rangle \\ & + [\phi_1^{(e)}(x_1)\phi_2^{(g)}(x_2)]|eg\rangle - [\phi_2^{(g)}(x_1)\phi_1^{(e)}(x_2)]|ge\rangle. \end{aligned} \quad (9)$$

In the complementary sector $x_1 > x_2$ we would get the same form except for a global minus sign consistent now with the Bosonic character. The resulting Bosonic state is discontinuous at contact and cannot represent noninteracting Bosons. Comparing Eq. (9) with Eqs. (6,7), we may interpret the Bosonic function as the result of contact collisions between impenetrable atoms that interchange internal state and momenta, exactly as described before. In other words, Ψ_B is a Bosonic solution of the two-body Schrödinger equation with Hamiltonian (5), with an infinite wall for the triplet potential, whereas the singlet potential, in addition to the infinite wall has an infinitely narrow and deep well. Ψ_B represents the wave function only outside the narrow well. Figure 7 provides a pictorial representation of the last two terms in Eq. (9) within the sector $x_1 < x_2$.

D. Generalization for N atoms

We have in summary constructed a Bosonic wave function for a system of two particles subjected to contact interactions with internal state and momentum interchange, using a dual system of two noninteracting Fermions and the antisymmetric unit function. The generalization to N -atoms is straightforward. The state for N noninteracting Fermions with internal structure takes the form

$$\begin{aligned} \Psi_F(x_1, \dots, x_N) &= \frac{1}{\sqrt{N!}} \det_{n,j=1}^N \Phi_n(x_j) \\ &= \frac{1}{\sqrt{N!}} \sum_{b_1, \dots, b_N = g, e} \begin{vmatrix} \phi_1^{(b_1)}(x_1) & \dots & \phi_1^{(b_N)}(x_N) \\ \vdots & \ddots & \vdots \\ \phi_N^{(b_1)}(x_1) & \dots & \phi_N^{(b_N)}(x_N) \end{vmatrix} |b_1 \dots b_N\rangle, \end{aligned}$$

and

$$\Psi_B(x_1, \dots, x_N) = \mathcal{A}\Psi_F(x_1, \dots, x_N), \quad (10)$$

where

$$\mathcal{A} = \prod_{1 \leq j < k \leq N} \text{sgn}(x_k - x_j), \quad (11)$$

is the Bosonic solution of the time-dependent or stationary Schrödinger equation for the Hamiltonian

$$\hat{H}_{\text{coll}} = -\frac{\hbar^2}{2m} \sum_{j=1}^N \partial_{x_j}^2 + \sum_{1 \leq j < \ell \leq N} [v_s(x_{j\ell}) \hat{P}_{j\ell}^s + v_t(x_{j\ell}) \hat{P}_{j\ell}^t], \quad (12)$$

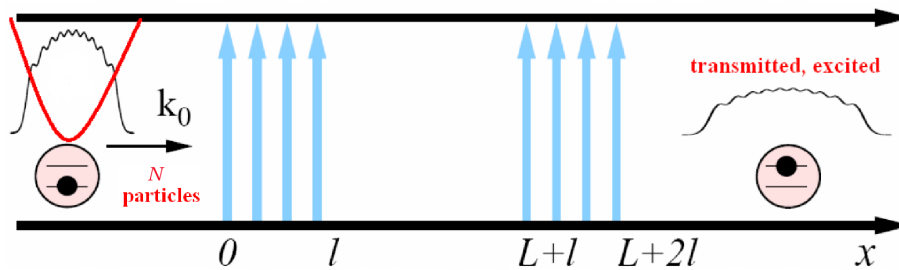


FIG. 8: Schematic setup for Ramsey interferometry of guided atoms in the spatial domain. The atoms are prepared in the ground state and the probability of excitation is measured after passing the two fields.

with the same contact interactions as before.

The density profile, normalized to N -particles, which gives the appearance of the cloud, is defined by

$$\rho_N(x) = N \int \|\Psi_B(x_1, \dots, x_N)\|^2 dx_2 \cdots dx_N. \quad (13)$$

Provided that the one-particle spinor states Φ_n are orthonormal, as they will always be hereafter, the density profile reads

$$\rho_N(x) = \sum_{b=g,e} \sum_{n=1}^N |\phi_n^{(b)}(x)|^2 = \sum_{b=g,e} \rho_N^{(b)}(x), \quad (14)$$

where the density profile for each of the channels defined by the two internal levels is given by

$$\rho_N^{(b)}(x) = \sum_{n=1}^N |\phi_n^{(b)}(x)|^2. \quad (15)$$

The simplicity achieved by our model parallels that of the usual (structureless) TG gas in the sense that an N -body wavefunction with interactions is obtained from freely-moving one-body states. Even more, this property is preserved by adding an interaction affecting the individual atoms only and coupling the internal levels. This is precisely the type of interaction that we find in the Ramsey interferometer.

III. THE RAMSEY INTERFEROMETER

Ramsey interferometry with guided ultracold atoms has recently been discussed in [11]. Here we consider a system of N two-level atoms in the Tonks-Girardeau regime, initially confined in their ground internal states in a harmonic trap of frequency ω . All energy scales are supposed to be much smaller than the transverse excitation energy $\hbar\omega_\perp$, so that the radial degrees of freedom are frozen out and the system is effectively one-dimensional. The cloud is prepared in the ground state, and released by switching off the trap along the x -axis at time $t = 0$ ($\omega = 0$ for $t > 0$); a momentum kick $\hbar k_0$ is also applied, so that the cloud moves along the x axis towards the two separated oscillating fields localized between 0 and l and between $l + L$ and $2l + L$ (Fig. 8). The initial state is prepared far from the first field. We thus have to take into account the spatial width (root of the variance) of the highest state, $\delta_N = [(N + 1/2)\hbar/(m\omega)]^{1/2}$, and choose the central initial position of the harmonic trap $x_0 < 0$ so that $|x_0| \gg \delta_N$.

In an oscillating-field-adapted interaction picture (which does not affect the collisional Hamiltonian) and using the Lamb-Dicke (see the next section), dipole and rotating-wave approximations the Hamiltonian is given, for each of the particles, by Eq. (1). For the explicit x dependence of $\Omega(x)$ we assume mesa functions, $\Omega(x) = \Omega$ for $x \in [0, l]$ and $x \in [l + L, 2l + L]$ and zero elsewhere. In addition, we have to include the interparticle interactions but this is done implicitly by means of the wave function (10) and its boundary conditions at contact.

The Ramsey pattern is defined by the dependence on the detuning of the probability of excited atoms after the interaction with the two field regions. From Eq. (15) it follows that $P_e = \frac{1}{N} \sum_{n=1}^N p_n^{(e)}$, which is a remarkably simple result for an N -body system with external and interparticle interactions. Once a particle incident from the left and

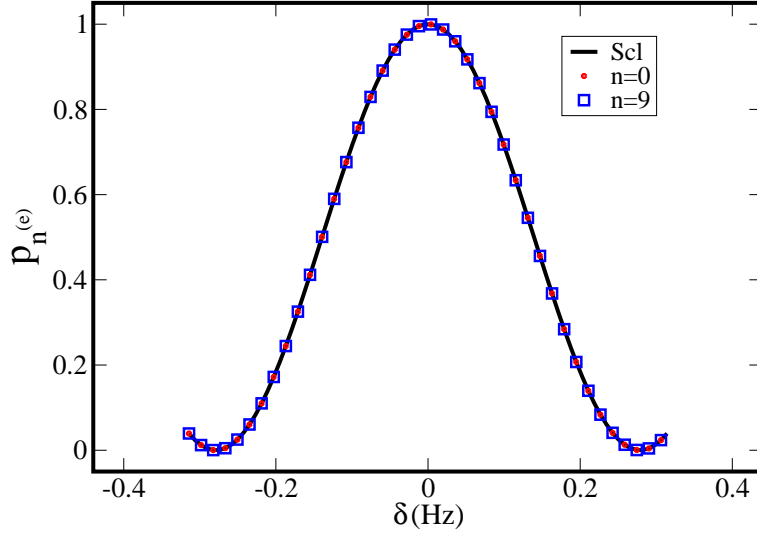


FIG. 9: Central fringe for Ramsey interferometry in the spatial domain. The agreement is shown for the $n = 0, 9$ single-particle wavepackets and the semiclassical result, for ^{133}Cs atoms, with $\hbar k_0/m = 1$ cm/s, $l = 1$ cm, $L = 10$ cm, $\delta_0 = 20$ μm ($\omega \simeq 0.6\text{Hz}$), and $t = 15$ s.

prepared in the state $e^{ik_0(x-x_0)}\phi_n(x-x_0)|g\rangle$ at $t = 0$ has passed completely through both fields, the probability amplitude for it to be in the excited state is

$$\phi_n^{(e)}(x, t) = \frac{1}{\sqrt{2\pi}} \int dk e^{iqx - ik^2 \hbar t / (2m)} T_{ge}(k) \tilde{\phi}_n(k), \quad (16)$$

where $\tilde{\phi}_n(k)$ is the wavenumber representation of the kicked n -th harmonic eigenstate,

$$\begin{aligned} \tilde{\phi}_n(k) &= \frac{(-i)^n}{\sqrt{2^n n!}} \left(\frac{2\delta_0^2}{\pi} \right)^{1/4} \\ &\times e^{-\delta_0^2 (k-k_0)^2} e^{-ikx_0} H_n[\sqrt{2}\delta_0(k-k_0)], \end{aligned} \quad (17)$$

the momentum in the excited state is $q = \sqrt{k^2 + 2m\Delta/\hbar}$, the spatial width of the $n = 0$ state is $\delta_0 = [\hbar/(2m\omega)]^{1/2}$, H_n the Hermite polynomials, and T_{ge} is the “double-barrier” transmission amplitude for the excited state corresponding to atoms incident in the ground state (the excited state probability for monochromatic incidence in the ground state is $\frac{q}{k}|T_{ge}|^2$). The full quantum treatment of T_{ge} can be done by means of the two-channel recurrence relations connecting it with one-field transmission and reflection amplitudes [11].

Our numerical simulations are for $l = 1$ cm, $L = 10$ cm, $N = 10$, and $v_0 = 1$ cm/s. Figure 9 shows that the variation of the excitation probability for different harmonic eigenstates is negligible in the scale shown, and in fact the curves for the central fringe are indistinguishable from the semiclassical result of Ramsey (which assumes classical motion for the center of mass, uncoupled from the internal levels),

$$\begin{aligned} P_{e,scl}(\Delta) &= \frac{4\Omega^2}{\Omega'^2} \sin^2 \left(\frac{\Omega'\tau}{2} \right) \left[\cos \left(\frac{\Omega'\tau}{2} \right) \cos \left(\frac{\Delta T}{2} \right) \right. \\ &\quad \left. - \frac{\Delta}{\Omega'} \sin \left(\frac{\Omega'\tau}{2} \right) \sin \left(\frac{\Delta T}{2} \right) \right]^2, \end{aligned} \quad (18)$$

where $\tau = l/v_0$, $T = L/v_0$, and $\Omega' = (\Omega^2 + \Delta^2)^{1/2}$.

There is in principle a broadening of the central fringe by increasing n due to the momentum broadening of vibrationally excited states. This effect may be expected however to be quite small for the few-body states of our calculations, $N = 10$, which is in fact of the order of current experiments with TG gases ($N \approx 15, 50$ in [20, 21]). The width (root of the variance) of the velocity distribution around the central velocity $v_0 = \hbar k_0/m$ for the n -th state is

$$\Delta_v = \left[\left(n + \frac{1}{2} \right) \frac{\omega \hbar}{m} \right]^{1/2} = \sqrt{2n+1} \frac{\hbar}{2m\delta_0}, \quad (19)$$

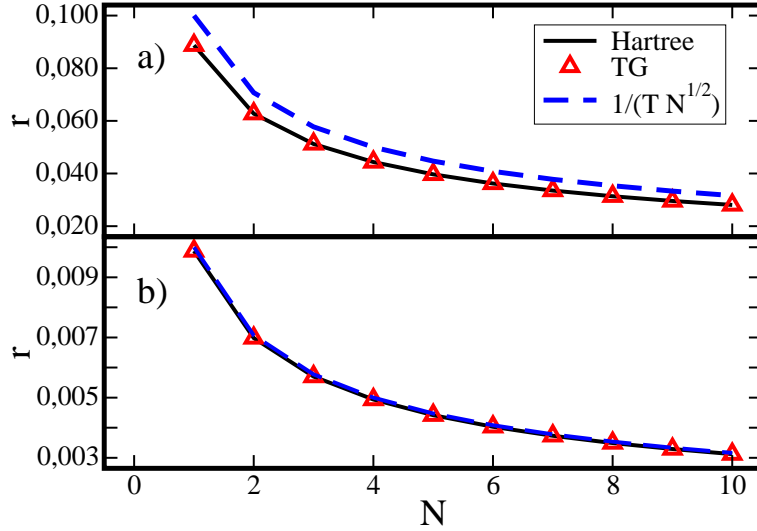


FIG. 10: Quantum projection noise ratio, Eq. (20), for the Ramsey interferometry in the spatial domain. The two-level Tonks-Girardeau gas ratio is essentially that of a Hartree product (uncorrelated atoms). The same parameters as in Fig. 9 are used, with a) $L = 10$ cm, b) $L = 100$ cm.

where we have used the spatial width of the $n = 0$ state, $\delta_0 = [\hbar/(2m\omega)]^{1/2}$. This will not affect significantly the width of the central fringe (proportional to the inverse of the crossing time T) as long as $\Delta_v/v_0 \ll 1$. For $v_0 = 1$ cm/s, $\delta_0 = 20\mu\text{m}$, the mass of ^{133}Cs , and $N = 10$, this ratio is $\sim 5 \times 10^{-3}$. N should be $\sim 4 \times 10^5$ to get a ratio of order one, but this means four orders of magnitude more particles than in the existing experiments.

We should also examine the quantum projection noise due to the fact that only a finite number of measurements are made to determine the excitation probability. The error to estimate the atomic frequency from the Ramsey pattern depends on the ratio [34]

$$r = \frac{\Delta S_Z}{|\partial \langle S_Z \rangle / \partial \delta|}, \quad (20)$$

which we calculate at half height of the central interference peak. r is theoretically smaller for the TG gas than for independent but for reasonable parameters the ratio r essentially coincides with that for freely moving, uncorrelated particles [34] and, for $L \gg l$ it gives $1/(T\sqrt{N})$ for all δ , see Fig. 10.

IV. RAMSEY INTERFEROMETRY IN THE TIME DOMAIN FOR GUIDED ATOMS

An alternative to the previous set-up is the separation of the fields in time rather than space but, at variance with the usual procedure, keeping the gas confined transversally at all times as required for the 1D regime of the TG gas, Fig. 11. Because of the tight confinement the transverse vibrational excitation is negligible so that the Ramsey pattern is given by the standard expression irrespective of the value of n . The whole TG gas therefore produces the usual Ramsey pattern (18).

V. SUMMARY AND DISCUSSION

Our model of a generalized Tonks-Girardeau regime suggests that very cold atoms may provide good atomic clocks if strongly confined. The advantages are: a very large time between field interactions; no collisional shifts; no velocity broadening; no instabilities as in BECs. More work is needed to ascertain the role of strongly interacting gases in interferometry and time-frequency metrology: to go from models to actual atoms, and to compensate or eliminate shifts due to confinement forces.

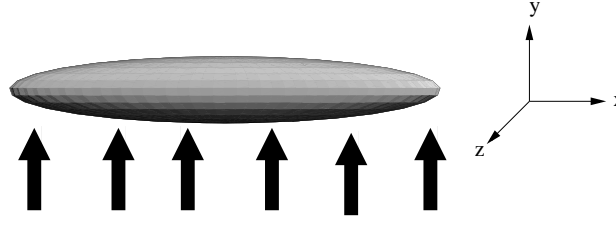


FIG. 11: Schematic setup for Ramsey interferometry in time domain. The TG gas is confined in a cigar-shaped trap and illuminated by a laser in y -direction.

Acknowledgments

We acknowledge discussions with M. Girardeau. This work has been supported by Ministerio de Educación y Ciencia (FIS2006-10268-C03-01; FIS2005-01369) and UPV-EHU (00039.310-15968/2004). S. V. M. acknowledges a research visitor Ph. D. student fellowship by the Ministry of Science, Research and Technology of Iran. A. C. acknowledges financial support by the Basque Government (BFI04.479).

References

-
- [1] Phillips W D 1998 *Rev. Mod. Phys.* **70** 721
 - [2] Laurent P *et al.* 1998 *Eur. Phys. J. D* **3** 201; Salomon C *et al.* 2001 *C. R. Acad. Sci. Paris Série IV* **2** 1313
 - [3] Wineland D J *et al.* 1992 *Phys. Rev. A* **46** R6797
 - [4] Huelga S F *et al.* 1997 *Phys. Rev. Lett.* **79** 3865
 - [5] Ramsey N F 1950 *Phys. Rev.* **78** 695; Ramsey N F 1956 *Molecular beams* (Clarendon Press, Oxford), Chapter V.4.
 - [6] Bordé C J 2001 *C. R. Acad. Sci. Paris Série IV* **2** 509; Wolf P *et al.* 2002 in *Proc. 6th Symp. on Frequency Standards and Metrology*, edited by P. Gill (World Scientific, 2002), p. 593; Bordé C J 2002 *Metrologia* **39** 435
 - [7] Bordé C J, Salomon C, Avrillier S, Van Lerberghe A, Bréant C, Bassi D, and Scoles G 1984 *Phys. Rev. A* **30** 1836
 - [8] Kasevich M and Chu S 1991 *Phys. Rev. Lett.* **67**, 181 (1991); 1992 *Appl. Phys. B* **54**, 321
 - [9] Morinaga A 1992 *Phys. Rev. A* **45**, 8019
 - [10] S. Schiller *et al.*, *arXiv:gr-qc/0608081*.
 - [11] Seidel D and Muga J G 2007 *Eur. Phys. J. D* **41** 71
 - [12] Harber D M, Lewandowski H J, Mc Guirk J M, and Cornell E A 2002 *Phys. Rev. A* **66** 053616
 - [13] Kadio D and Band Y B 2006 *Phys. Rev. A* **74** 053609
 - [14] Girardeau M D 1960 *J. Math. Phys.* **1** 516
 - [15] Girardeau M D 1965 *Phys. Rev.* **139** B500, Secs. 2, 3, and 6.
 - [16] Olshanii M 1998 *Phys. Rev. Lett.* **81** 938
 - [17] Bergeman T, Moore M G, and Olshanii M 2003 *Phys. Rev. Lett.* **91** 163201
 - [18] Petrov D S, Shlyapnikov G V, and Walraven J T M 2000 *Phys. Rev. Lett.* **85** 3745
 - [19] Lieb E H and Liniger W 1963 *Phys. Rev.* **130** 1605
 - [20] Paredes B *et al.* 2004 *Nature* **429** 277
 - [21] Kinoshita T, Wenger T R, and Weiss D S 2004 *Science* **305** 1125
 - [22] Kaplan A, Andersen M F, and Davidson N 2002 *Phys. Rev. A* **66** 045401
 - [23] Haffner H *et al.* 2003 *Phys. Rev. Lett.* **90** 143602
 - [24] Girardeau M D and Wright E M 2000 *Phys. Rev. Lett.* **84** 5239
 - [25] Girardeau M D, Das K K and Wright E M 2002 *Phys. Rev. A* **66** 023604
 - [26] Girardeau M D, Nguyen H, and Olshanii M 2004 *Optics Communications* **243** 3
 - [27] Girardeau M D 2006 *Phys. Rev. Lett.* **97** 210401
 - [28] Yang C N 1967 *Phys. Rev. Lett.* **19** 1312; Gaudin M 1967 *Phys. Lett. A* **24** 55; Guan X W *et al.*, *cond-mat/0702191*.
 - [29] Girardeau M D and Olshanii M, *cond-mat/0309396*.
 - [30] Girardeau M D and Olshanii M 2004 *Phys. Rev. A* **70** 023608
 - [31] Cheon T and Shigehara T 1998 *Phys. Lett. A* **243**, 111; 1999 *Phys. Rev. Lett.* **82** 2536
 - [32] Yurovsky V A and Band Y B 2007 *Phys. Rev. A* **75** 012717
 - [33] Granger B E and Blume D 2004 *Phys. Rev. Lett.* **92** 133202

- [34] Itano W M *et al.* 1993 *Phys. Rev. A* **47** 3554
- [35] Reichel J and Thwissen J H 2004 *J. Phys. IV France* **116** 265 (2004).
- [36] Gangardt D M and Shlyapnikov G V 2003 *Phys. Rev. Lett.* **90** 010401
- [37] del Campo A, Muga J G, and Girardeau M D, arXiv:0705.0937, *Phys. Rev. A*, accepted.
- [38] M. Girardeau, arXiv:0707.1884